Pleistocene periglacial imprinting on polygenetic soils and paleosols in the SW Italian Alps

Michele E. D'Amico*[1], E. Pintaldi[1], M. Catoni[1], M. Freppaz[12], E. Bonifacio[1]

[1]Università degli Studi di Torino, DISAFA, Via Leonardo da Vinci 44, 10095 Grugliasco (To), Italy.

[2]Università degli Studi di Torino, NATRISK, Via Leonardo da Vinci 44, 10095 Grugliasco (To), Italy.

*corresponding author: ecomike77@gmail.com

Abstract

Because of extensive Pleistocenic glaciations, which erased most of the previously existing soils, slope steepness and climatic conditions favoring soil erosion, most soils observed in the Alps (and in other mid-latitude mountain ranges) have developed during the Holocene or Late Glacial period. However, in few sites, particularly in the outermost sections of the Alpine range, Pleistocene glaciers covered only small and scattered surfaces, and ancient soils could be preserved for long periods on stable surfaces. In many cases, these soils retain good memories of Quaternary periglacial activity, which have never been characterized on the Alpine range. Based on both geomorphological and pedological interpretations, this work aims to investigate these environments, providing, therefore, new evidences to support paleoclimate reconstructions on the Alps.

We described and sampled soils on stable surfaces in the Upper Tanaro valley, Ligurian Alps (Southwestern Piemonte, Italy). The sampling sites were between 600 to 1600 m a.s.l., under present day lower montane *Ostrya carpinifolia*, montane *Fagus sylvatica* forests or montane heath/grazed grassland, on quartz-rich substrata.

The surface morphology often showed strongly developed fossil periglacial morphologies such as large-scale patterned ground, blockfields/blockstreams or solifluction sheets.

The soils preserved in such Quaternary periglacial landforms normally showed stratification of different layers (units), separated by structural discontinuities, evidencing different depositional settings and different pedogenic development degree. A strong cryogenic granulometric sorting characterized all the observed soils/paleosols, with silt-enriched horizons and lateral differentiation of sand- and stone-rich parts and fine enriched ones; organic matter was irregularly distributed at depth as a result of past cryoturbation. Compact and dense layers with strong platy/lenticular structural aggregation, wedge casts and large-scale cryoturbations were described below fixed depths in all soil profiles.

Thus, surface morphology and soil properties suggest the presence of permafrost during cold Pleistocene phases, with two main active layer thicknesses at 60-120 and 100-160 cm depths respectively.

Keywords: Alps; paleoenvironmental indicators; fossil periglacial processes, cryoturbation; relict podzols

1. Introduction

Cryogenic processes often leave durable traces in soils affected by deep seasonal frost or permafrost during their existence and many morphological and micromorphological characteristics indicate cryoturbation, also in places where these processes have been inactive for many thousands of years. Soil cryoturbation is due to frost heaving caused by the formation of ice lenses, which in turn is related to frost susceptibility (controlled by texture, porosity and organic matter content) and to the drainage condition. Cryoturbations are indicative of cold and humid climate, but not always of permafrost conditions (Van Vliet- Lanoë, 1998). Cryoturbation is also reflected by surface topographical features, such as patterned ground, blockfields and blockstreams, stone-banked solifluction and gelifluction lobes and sheets.

Because of their high stability on certain poorly weatherable lithologies, many soil and surface morphological indicators have been used in paleoclimatic reconstructions, as their formation can be associated with specific environmental conditions (e.g., Karte, 1983) even if temperature thresholds for each feature are mostly empirical and lack precise justifications (Murton and Kolstrup, 2003). The main drawback to the use of present-day analogues to fossil periglacial soil/landforms is represented by the impossibility to obtain present day analogues to severe Pleistocene conditions in mid-latitude areas, given the higher precipitation rate and the difference in solar radiation between mid and high-latitude environments, where periglacial activity is active at present. High altitude mountains might represent a better comparison, but many of the large-scale periglacial morphologies, often observed as Pleistocene legacy of cold periods, have not been described as presently active in mid-latitude, high-altitude areas. The assemblage of different cryogenic features developed apparently during the same period could give, however, insights on the overall severity of the period, as the environmental constraints of single features remain unsure.

The extent of Pleistocene permafrost in Northern Italy is largely unknown. Differently from most of Central Europe (Vandenberghe and Pissart, 1993), clear indicators of permafrost are absent. In fact, Cremaschi and Van Vliet-Lanoë (1990) stated that no permafrost ever reached the Po plain, being developed only above 800-1000 m a.s.l. (Van Vliet- Lanoë, 1998). However, blockstreams and blockfields are located at lower altitudes, such as in the Complesso di Lanzo (Western Alps) down to 450 m a.s.l. (Fioraso and Spagnolo, 2009), or in the Beigua Massif (Ligurian Alps) down to 650 m a.s.l. (Firpo et al., 2006; Rellini et al., 2014), while traces of possible permafrost during the LGM (Last Glacial Maximum) have been detected in caves close to the Mediterranean coast of Liguria at

(present day) 90 m a.s.l. (Rellini et al., 2013). Permafrost indicators have been observed also in mountain soils at much lower latitudes in Calabria, Southern Italy, at a relatively low altitude (Dimase, 2006). The Pleistocene record in the Alps is dominated by glaciations and glacial forms, but periglacial traces are also preserved in unglaciated terrains, even if seldom studied (e.g., Rellini et al., 2014).

The lack of knowledge of the distribution, morphologic characteristics and climatic implications of fossil periglacial landforms, and of soils developed in them, represents an important gap in the paleoclimate understanding in the Alps. The knowledge of the overall severity of periglacial conditions during Pleistocene glacial phases could help to better hypothesize the southern boundary of permafrost in an area which is still debated (e.g. Cremaschi and Van Vliet-Lanoë, 1990, Rellini et al. 2013).

We thus documented the existence of extensive Pleistocene periglacial landforms and described the associated soils and paleosols, in unglaciated Alpine terrains, in order to 1) obtain indications on the severity of periglacial conditions able to support paleoclimate reconstructions, and 2) detect pedogenic processes active during periglacial conditions or warmer interglacials. To these aims we used geomorphological features and soil morphological and textural properties.

2. Regional setting and study area

The ELA (Equilibrium Line Altitude) in the Western Alps during LGM was around 1850-2000 m a.s.l. (Federici et al., 2012), thus Pleistocene glaciers occupied only small and scattered cirques above 1700-2000 m a.s.l. in the Ligurian Alps (Piemonte, NW Italy) (Vanossi, 1990; Carraro and Giardino, 2004). The geomorphology is here dominated by long term tectonic uplift, river incision, temporary peneplanation and cryoplanation during cold Quaternary periods (as in nearby areas described by Firpo et al., 2006; Paro, 2011; Rellini et al., 2014). All the geomorphic features derived from these processes are particularly well preserved in the Upper Tanaro Valley (Fig. 1), where a series of relict surfaces (uplifted bedrock valley floor remnants and cryoplanation surfaces) are easily recognizable as flat or gently sloping summits and plateaus perched high above the present-day valley floor, at different altitudes on the north and south slopes because of differential tectonic uplift. On these gently sloping plateaus and erosion terraces, present-day erosion and deposition processes are very limited.

The studied relict surfaces and slopes show many evidences of Pleistocene fossil periglacial morphologies (table 1). Morphologic indicators of relict preglacial or Early Quaternary surfaces (Goodfellow, 2007), such as blockfields and tors derived from in situ deep weathering and frost shattering of the bedrock (Ballantyne, 2010), are widespread on many of the considered surfaces

and on the nearby slopes. Many flat or undulating surfaces on hard quartzitic conglomerate are covered by blockfields, which included better vegetated areas with well-preserved patterned ground features, mostly sorted circles. Sorted circles have a 2-5 m diameter, and are overgrown with a thick grassland/heath vegetation. They have stony rims composed of large, lichen-covered subrounded boulders, with diameter up to 50-150 cm. The circle rims are often sunken below the vegetation-covered central part and are clast-supported down to 70-100 cm of depth; below this depth, the stone content sharply decreases. The rims have imbricated stones down to a depth of ca. 40 cm, while they are verticalized below.

Lobate solifluction terraces with a ca. 1 m thick riser are preserved on most gently sloping slopes (between 5° and 15°), while blockstreams and blockslopes are preserved, particularly on the hardest quartzites. On more easily weatherable gneiss, unsorted stripes are not visible below the vegetation cover but evidences are visible in road cuts as repeated patterns of stone-rich sectors or of different pedogenic horizons. Stratified slope deposits (grèzes litées, Karte, 1983) are preserved as well, on slopes now covered by beech forests with *Rhododendron ferrugineum* understory.

Many of these periglacial relict morphologies can be used to infer permafrost/intense frost conditions (table 2).

A precise chronology of the geomorphic events leading to the formation of the relict surfaces is missing, but in other portions of the Ligurian Alps, some 50 km east from our study area, remnants of analogous relict surfaces perched some hundreds of meters above the valley floors were considered fragments of Pliocene alluvial terraces (Rellini et al., 2014). Polygenetic soils on some relict surfaces showing weaker periglacial morphologies were characterized by repeated cycles of strong pedogenesis, sometimes with evidences of subtropical climates, and cryoturbation (D'Amico et al., 2016).

We thus explored such surfaces, described and sampled in detail 7 well developed soil profiles, chosen amidst a much larger number of observations because of their good state of preservation and high degree of pedogenic development. The main environmental properties of the sampling sites are shown in Table 1. A range of different rock types are the lithological parent material, ranging from coarse quartzitic conglomerate, to gneiss and silica-rich shales (Vanossi, 1990).

Present day land use is montane *Fagus sylvatica* L., submontane *Ostrya carpinifolia* Scop. forests or grazed grassland colonized by heath species and *Rhododendron ferrugineum* L. (Table 1). The average annual temperature ranges between 4° and 8°C, decreasing with altitude and with local variability caused by slope aspect. The annual precipitation is around 800-1200 mm, with spring and fall maxima and summer minima (Biancotti et al., 1998). Normally, water scarcity is never a limiting factor for plant growth (udic moisture regime), even during the rather dry summer months

(average July rainfall is around 40 mm). Summer fogs are common, thanks to the proximity with the Mediterranean Sea, and increase available moisture in the surface soil layers. Snow cover normally lasts from December to March/April in the considered altitudinal range, but snow cover is not very thick because of frequent winter rain-on-snow episodes associated with warm Mediterranean air masses.

3. Methods

At each selected site, a cross section of a whole large-scale cryogenic feature (such as sorted or unsorted patterned ground or solifluction lobe) was opened, showing a complex soil profile described according to the FAO guidelines (FAO, 2006). In this work, we used qualifiers in brackets in horizon designation to indicate minor but detectable characteristics. The soil samples were taken from the whole thickness of the genetic horizons, air dried, sieved to 2 mm and analyzed. Undisturbed 100 cm^3 samples were collected (where possible) in steel cores for the bulk density calculation; the stones were excluded from the considered volume, and their weight subtracted,. The analyses followed the methods reported by Van Reeuwijk (2002). pH values were measured in a 1:2.5 soil-water suspension. The total C concentration was measured by dry combustion with an elemental analyzer (CE Instruments NA2100, Rodano, Italy); given the absence of carbonates in extremely acidic podzolized soils, the total C content corresponded to organic carbon (TOC). The particle size distribution was determined by the pipette method after treating the samples with H_2O_2 and dispersing with Na-hexametaphosphate. Dithionite-extractable and total Fe (Fed and Fet respectively) were extracted in some samples in order to obtain indications about soil weathering.

The degree of development of each soil profile was determined through the application of the Profile Development Index (PDI), following the approach outlined by Harden (1982) and Harden and Taylor (1983). The PDI is based on field description and represents a semi-quantitative tool to measure the amount of pedogenic change occurred in time, since parent material was deposited. For each soil, a Cr horizon of appropriate lithology was used, even if the parent material was not reached in most cases. Considering the high adaptability of the method (Schaetzl and Thompson, 2015), we selected and combined specific parameters for each type of horizon (see table 3), according to their morphologic/diagnostic properties. Furthermore, as most soil profiles were characterized by the podzolization processes, we introduced in the PDI calculation the POD index (Shaetzel and Mokma, 1988) and the E contrast index. The latter was specially created for eluvial/Albic horizons, and it is based on the color contrast between each E horizon and the best developed Bs/Bhs associated to it. It is calculated as the sum of hue and value decrease, and chroma

increase in respect to the Bs, attributing 10 points for each step from red to yellow, 10 points for each decrease in value and 10 for increase in chroma.

In addition, the obtained values were compared with the modified PDI calculated on some soil profiles close to the study area, developed on surfaces not showing any Pleistocene periglacial features (Catoni et al., 2016) and with paleosols on flat relict surfaces (D'Amico et al., 2016).

4. Results

4.1. Soil morphology, structure, Pleistocene and Holocene pedogenic trends and development degree

The studied soils were characterized by polygenesis, with different soil characteristics associated to different environmental conditions. Except D1, showing a Mollic A horizon, the upper part of all profiles was characterized by different degrees of podzolization (Electronic Annex). Umbric horizons were developed under pastures above E and Bs horizons, while A horizons were absent or weakly developed below heath or forest vegetation. Below these surface layers, a large array of cryostructures and pedogenic evidences of Pleistocene cold periods was observed (table 4), in relation with slope steepness and, secondarily, with parent material lithology.

The modified PDI index (table 5) evidenced a strong development degree of the considered soil profiles, ranging between 31 and 64. The values obtained from many profiles (S4, S5, and S11) are underestimated because the thickness of the deepest genetic B or A/E horizons is unknown. Where separate soils were superimposed on each other because of relict periglacial solifluction and gelifluction (S4, S11, and S13), the surface soil, likely developed during the Holocene, often had a lower pedogenic development than deeper ones, ranging between 10 and 16.

4.1.1. D1 – fragipan soil

Soils with fragipan (Eutric Skeletic Fragic Retisol (Loamic)) were preserved at the lowest altitude (ca. 730 m a.s.l.), developed in slope deposits on weatherable silica-rich shales on northward aspects (fig. 2a). Large blockslopes, tors and fossil rock glaciers on nearby quartzitic outcrops evidence the existence of Quaternary periglacial conditions. Below a surface layer (Mollic horizon), ca. 40 cm thick, the thick fragipan (down to 180 cm) was characterized by all the diagnostic properties required by IUSS Working Group (2015), i.e. coarse platy aggregation, hard consistence that impedes root penetration and water infiltration, very fast slaking of air-dried aggregates in water. Whitish vertical streaks interrupt the homogeneity of the yellowish-brown horizon, and greyish mottles surround the coarse platy and lenticular aggregates; black Fe-Mn coatings covered a few aggregate faces as well. Only thin clay coatings were visible on the aggregate faces in the field.

208 The density was around 1.75 g cm^{-3}, which is a much higher value compared to the 1.0-1.3 g cm^{-3}
209 measured in the overlying loose A horizon. The weakly weathered stone fragments in the upper
210 layer displayed no specific orientation thanks to bioturbation by earthworms and pedoturbation,
211 while in the fragipan horizon they were mostly oriented parallel to the slope, and highly weathered.
212 This soil showed weakly acidic pH values and a quite high proportion of pedogenic Fe-oxides
213 (Fed/Fet), but no significant variations among the different surface A or subsurface fragipan
214 horizons (Electronic Annex).
215
216 **4.1.2. S18 – Degraded Podzol with ortstein and fragipan layers**
217 On gently sloping surfaces (< 7°) on quartzite, well developed Podzols (Retic Albic Ortsteinic
218 Podzol (Fragic, Hyperspodic)) were preserved, showing different units separated by structural
219 discontinuities (fig. 2b):
220 - Unit 1: 30 cm thick A and AE horizon sequence, without preferential orientation of stones, and
221 soft consistence, with a lower wavy boundary.
222 - Unit 2: down to 95 cm of depth, this layer included a E-Bs/E sequence of pedogenic horizons;
223 these horizons were characterized by hard consistence, high vesicular porosity, thick silt caps
224 and stone fragments oriented parallel to the slope angle; the degraded Bs/E horizon (fig. 2b)
225 was characterized by a reticulate pattern (retic properties) in which coarse Bs aggregates, more
226 or less of cubic shape, were surrounded by a net of albic materials, which evidenced the
227 degradation pathway of the Bs horizon. An abrupt structural discontinuity was observed at ca.
228 95 cm.
229 - Unit 3: down to 180 + cm, composed of Bsm, Btsx, Crtx horizons; the top 30 cm were
230 cemented by spodic materials (Ortstein), while between 125 and 180 cm the hard but more
231 brittle consistence and the quick slaking in water evidenced fragic properties. The main
232 characteristic of this layer was the coarse and well defined platy and lenticular structure and a
233 high compaction. The platy and lenticular aggregates were separated by smooth pressure faces
234 sometimes including coarse pores. These coarse pores were partially filled with small rounded
235 silty aggregates and tiny stones, grading into hard and compact silt caps. Reddish clay coatings
236 were also visible on the faces of the aggregates.
237
238 **4.1.3. S5 – Soils in sorted patterned ground**
239 On flat surfaces, trenches cut across large sorted circles and their stony border evidenced complex
240 soils (Skeletic Umbric Entic/Albic Podzol (Abruptic, Loamic, Densic, Relictiturbic)), showing the
241 typical internal morphology of sorted patterned ground soils. In particular, stone-rich sectors

showed thick sandy E horizons down to ca. 90 cm (fig. 3a, 3b). The well vegetated central parts were rich in fine materials, despite the resistant quartzitic parent material (fig. 3c). Two unconformities were observed in the central, fines-rich sector, separating three morphologic units:

- Unit 1 – 0-45 cm: this unit was characterized by a weak present-day podzolization (well-developed Bs but only thin and discontinuous E horizons), with Umbric epipedon; the structure was granular, biogenic, in the thick A horizon (probably because of the anthropogenic grassland use) and subangular blocky in the Bs; stone fragments were horizontal.
- Unit 2 – 45-90 cm: a rather abrupt but wavy structural (thaw) unconformity separated this unit from the one above. Unit 2 was characterized by a brown color (7.5YR 5/4) and a coarse platy/lenticular structure, with thick siltans, compression caps and small granular silty aggregates in large pores between the aggregates. Inside the aggregates, vesicles were observed. The density and compactness were very high (field moist samples could be broken only after a strong pressure).
- Unit 3 – 90-105+ cm: a more or less horizontal Placic horizon evidenced the structural discontinuity with the unit above, below which a very compact, stone- and sand-rich layer (Electronic Annex) was observed, enriched in Fe-Mn cemented, spherical and thinly layered pisoliths and soft concentrations. The structure was coarse lenticular. This unit extended almost parallel to the surface, also below the thick sandy E horizons below stony rims.

4.1.4. S11-S13 – Soils in fossil unsorted stripes on slopes

Strongly polygenetic soils also characterized fossil unsorted stripes on slopes (Albic Podzol (Loamic, Densic, Ruptic, Relictiturbic)). They comprised three units separated by morphologic and structural discontinuities. Fig. 4a and fig. 5a represent profiles S11 and S13 respectively, including some of their specific features. In particular:

- Unit 1 – the surface layer developed in 60-110 cm thick solifluction sheets (fig. 4a, 5a and 5e). Holocene pedogenesis normally led to the formation of Podzols with various degrees of development: in S11 the central part was an E horizon in genetic continuity with the one observed in Unit 2, but softer. Stone fragments (fig. 4b, 5b) were randomly oriented and no platy aggregates were detected, thus this layer can be considered a gelifluction sheet (Van Vliet-Lanoë 1985).
- 1-2 discontinuity – abrupt and parallel to the surface, this discontinuity separated present-day soils from buried ones. In S11, a dark, 1-2 cm thick layer characterized by illuvial organic matter associated with a large density increase (fig. 4d, Electronic Annex) was observed across

the whole section. This horizon might represent an accumulation of organic carbon associated with the presence of a temporary permafrost table (Gubin and Lupachev, 2017).

- Unit 2 – In this layer, dominated by cryoturbations, strongly developed Podzols (paleosols) were usually preserved, whose horizons were distorted, convoluted and laterally disrupted with dislocated patches. Drop-shaped involutions with flat bottoms were observed, mainly constituted of E or EA strongly weathered, fine materials. The density in these involutions was very high (average values around 1.7 g/cm^3 when measurable), while the surrounding materials had an average bulk density of 1.4 g/cm^3 when measurable (fig. 4d, 5d). Drop-shaped involutions brought dislocated silty E or A horizons down to the 2-3 discontinuity, and they were characterized by a well-developed platy structure. Patches of organic C-rich surface horizons, thinly alternated with layers of E and Bs ones, were observed in S13, right above the deepest (2-3) discontinuity at the bottom of drop-shaped involutions (fig. 5f, 5g), and in S11 near verticalized stones at the limit between the large involutions and the surrounding matrix. Abundant charcoal fragments were also detected in deep layers, evidencing strong mixing. Thick, hard silt caps on the upper stone faces were common as well. The drop-shaped involutions involving fine-textured E and AE horizons are compatible with a positive gradient of frost susceptibility, i.e. highly frost susceptible loamy E horizons expanding above more sand and stone-rich Bs ones (Van Vliet-Lanoë 1998). The compaction and high bulk density increase in involutions can be related with thaw collapse of ice rich materials. In one case (S11), a 30-40 cm wide wedge cast was preserved as well, characterized by high content of verticalized stones, loose consistence and much higher silt content (45.3%) than the surrounding compact and denser materials (28-33%, fig. 4a, 4c).
- Unit 3 – Below a sharp discontinuity at around 160 cm of depth, this layer was characterized by high density, high stone contents and a coarse platy/lenticular structure with visible, abundant vesicular pores. In S13, this layer was rich in coarse sand, and it was characterized by a generalized weaker weathering degree of the material (3C@ horizon). 3E/A horizons, belonging to another Podzol cycle, were preserved in the other case (S11).

4.1.5. S4 – Soils in thick stone-banked solifluction lobes

On some sloping surfaces covered by thick solifluction lobes, strongly polygenetic soils (Hyperskeletic Umbric Albic Ortstenic Podzol (Densic, Ruptic, Hyperspodic Relictiturbic)) were characterized by a similar stratification as soils in unsorted stripes, separated by structural discontinuities with a parallel orientation to the slope (fig. 6a). In particular, they showed:

- Unit 1 - surface layer developed in solifluction sheets. This layer was 75 cm thick and was characterized by oriented stones parallel to the slope surface and a switch from matrix-supported to clast-supported towards the bottom. Holocene pedogenesis normally led to the formation of Podzols and Umbrisols with a various degree of development, as visible from the horizon sequence in fig. 6a. The lower 30 cm had very hard consistence, abundant porosity and strong platy structure, with thin (3-6 cm thick) layers characterized by extremely high gravel content (up to 95% in volume) alternated to thin silt-rich layers. Well preserved vesicular porosity was observed inside the silt-rich aggregates, while stone-rich aggregates were mostly clast-supported with voids in between. Thick and hard silt caps were also observed on the upper face of the stone fragments.
- 1-2 discontinuity – below the hard layer, remnants of a soft, biogenic granular buried A horizon are preserved, morphologically resembling a present-day Mollic horizon with structural aggregates created by earthworm activity. This horizon is particularly well preserved in the cryogenic convolutions and in the soil wedge (see the description of Unit 2).
- Unit 2 – In this layer, dominated by cryoturbations, thick Bsm and Btsm horizons were preserved. A Placic horizon represents the upper limit of this layer, which was distorted, and locally convoluted with small drop shaped inclusions (20 cm long, 3-4 cm wide). A soil wedge cast is also observed, traversing the whole layer down to ca. 155 cm and filled with the soft, organic matter-rich Mollic A material forming the 1-2 discontinuity. A much higher silt content, compared to the surrounding materials, characterized this infilling as well (fig. 6b). As the wedge cast was buried under Unit 1 (dense solifluction material), no polygons were visible on the surface, but it linearly extended uphill for at least more than 1 m without losing its shape, which is one of the requirements for wedge cast recognition (Ballantyne and Harris, 1994).
- 2-3 discontinuity (thaw unconformity), sharp and almost parallel to the slope; it was located at a depth of around 155 cm.
- Unit 3 – This layer was characterized by a high density (higher than 1.7 g/cm^3, when measurable), a coarse granulometry with high stone and coarse sand content, and a strong coarse platy/lenticular structure. A 2-3% of small Fe-Mn nodules was observed, with the highest concentration close to the upper boundary.

4.1.6. S12 – Soils in stratified slope deposits (grezes litees)

One of the studied soils (Hyperskeletic Glossic Umbric Hyperalbic Ortstenic Podzol (Densic, Ruptic, Hyperspodic, Relictiturbic) was developed in a stratified slope deposit, located on the edge of a gentle slope below a tor-dotted ridge.

- Unit 1 – it represented the upper 1 m and was developed in gelifluction unsorted material, where stone fragments were mostly randomly oriented. It was characterized by a particularly strong Holocene podzolization (E horizons up to 1 m thick). Bhs and Bsm horizons were only locally observed in the surface layer (fig. 7a), but were mostly developed below the underlying discontinuity. Horizontally, Bs, Bhs and Bsm horizons were discontinuous and were alternated with C or E vertical bands crossing the whole profile (fig. 7a).
- 1-2 discontinuity - The lower limit of the gelifluction layer was characterized by a 5 cm thick, silt-enriched horizon characterized by strong platy structure, high density (1.72 g cm^{-3}) and abundant vesicular porosity.
- Unit 2 was observed below this silty layer, characterized by an alternation of stone- or silt-rich layers (fig. 7b), with a wavy lateral trend. Silty layers were all dense and rich in small vesicular pores, with thin laminar aggregation, while stone-rich layers were mostly clast-supported and characterized by clast orientation and very little fine-earth fraction (less than 10%). Discontinuous Placic horizons were observed above silty laminar layers in the spodic bands. Organic matter-rich layers were preserved below 2.2 m, where remnants of plant-derived fibers were mixed with angular and aligned stone fragments, probably corresponding to an ancient topographic surface buried by solifluction processes inside the laminated slope deposit (Unit 3).

Dense silty and laminar horizons strongly reduce water percolation through the soils, and after strong rainfall events water tends to flow above them. Lateral water movement could be implicated in the development of the E/EC – Bs/Bsm/Bhs vertical bands. The thick E horizon, unusual in temperate areas, could be the results of pedogenesis on pre-weathered materials, mixed by periglacial solifluction phenomena (Prosser and Roseby, 1995).

4.2.Granulometric differentiation

In many soils, a strong textural and granulometric differentiation was measured amidst different horizons and different sectors, both laterally and vertically.

The largest granulometric differentiation was observed in sorted patterned ground soils, with stones accumulated close to the stony rims and in the dense basal horizons (fig. 3b), as typical in sorted patterned ground (Ugolini et al., 2006). Below stony rims in sorted circles (S5), stone content

sharply decreased below 70-120 cm. The coarsest stones were in the surface layers, but some verticalized large ones were also rooted in the deep, dense Bs, 2Bts and 3Bsc horizons (fig. 3a). The highest silt (up to 45%) and clay contents (up to 27%, Electronic annex) were measured in Bs horizons developed in the central part, while the thick E horizons under the stony borders were loamy-sandy (fig. 3b, 3c, with silt content below 25% and clay below 10%). Another silt-rich layer was the thin platy horizon above the lowest discontinuity (up to 40% also below the loamy-sandy materials below the rim). The boundary between the fine central part and the loamy-sandy one was rather abrupt. In the central, fines-enriched sector, silt cutans were thick and well visible in the Bts horizon located at a depth between ca. 45 and 80-90 cm, below an abrupt linear boundary separating this horizon from the overlying Bs one; small rounded silty aggregates were well visible in the pores separating the coarse lenticular aggregates. Below this layer, no visible siltans were recognized. Below the deep unconformity at ca. 90 cm, the texture was sandier than above.

A very large differentiation in stone content, both laterally and vertically, was visible also in the subsurface heavily cryoturbated layers in unsorted patterned ground soils, despite the lack of any surface evidence (S11, S13). In these cases, stone contents ranged between 50-70% in Bs@ horizons and 2-10% in drop-shaped E@ inclusions. In these soils and paleosols, silt contents ranged between ca. 20-25% and 50% in contiguous horizons in the intermediate, heavily cryoturbated layers (Unit 2). In particular, the highest silt contents were measured in E horizons, while the highest sand and stone contents in the Bs ones (fig. 4b, 5c). Another silt-enriched layer was detected close to the 1-2 discontinuity, where the thickest and most compact silt caps were observed.

Dense layers and fragipans were not associated with particular granulometric variations, but thick silt caps and small rounded silty aggregates in pores were observed on the upper faces of the hard lenticular aggregates. Dense concentrations of fine stones and coarse sand were sometimes observed below the same stones.

5. Discussion

5.1 Soil and surface indicators of periglacial conditions

Soil and surface morphological indicators of periglacial conditions are useful in paleoclimatic reconstructions, but it is only through the combined use of several periglacial forms that some attempt to link them to specific climatic indicators can be attempted.

As often observedMany periglacial indicators were preserved in the study area, mostly on hard quartzites and quartzitic conglomerates, as often observed on such hard and weakly weatherable rocks (e.g., Clark and Ciolkosz, 1988; André et al., 2008), but also on more easily weatherable gneiss and shales.

In particular, fossil surface morphologies indicative of cold climate/permafrost conditions were widespread (table 2).

As many different geomorphic indicators of permafrost are preserved in the same geographic area over small distances, severe permafrost conditions were highly probable during long periods across the Pleistocene (as in Rellini et al., 2014).

The observed soils, developed and preserved in or near some of these fossil periglacial landforms, were thus strongly influenced by Quaternary cold periods, and are characterized by a wide array of cryoturbation features, that point to the presence of permafrost for long periods during soil development and may help to hypothesize the thickness of the active layer.

In particular:

- ice wedge casts (MAAT < -4/-8°C), sand wedges, (MAAT < -4/-8°C in dry conditions) and soil wedges (MAAT <1°/-1°C) (Van Vliet-Lanoë, 1991; Matsuoka, 2011), observed in S4 and S11, indicate severely cold climates, with the lowest temperature values valid for coarse materials (Ballantyne and Harris, 1994); shallow soil wedges indicate at least deep seasonal freezing, while the other casts indicate permafrost. The huge uncertainties about the present-day conditions necessary for wedge formation and development are however still existing (Murton and Kolstrup, 2003). Frost cracks developed in mountain areas are active, or have been active during the Holocene, at MAAT < -3°C in continental climates, such as on the Colorado Front Range, possibly caused by processes of differential frost heave (Benedict, 1970, 1979). Tree-fall features are less likely as the observed wedges extended for more than one meter uphill along the slope direction, while the shape of tree-fall pits are usually irregularly shaped (Šamonil et al., 2015). Relict patterned ground features could be hidden below the surface solifluction materials.
- Dense horizons (S4, S5, S11, S13) or fragipans (D1, S18) with thick platy aggregation and an abrupt upper boundary may indicate permafrost condition and their position is related to the depth of the active layer (Fitzpatrick, 1956, Van Vliet-Lanoë, 1991, 1998). These structures are normally associated with the transient layer, which is the ice-rich layer in the upper part of the permafrost that undergoes multiannual cycles of melting and aggradation (French and Shur, 2010) resulting in the formation of thick ice lenses. Even if our soils only seldom show typical fragipan horizons (D1, S18), the deep non-cryoturbated layers (Unit 3 in slope soils) have a coarse platy structure, an abrupt upper boundary and are often compact, dense, hard when dry, friable when moist and with dry aggregates slaking in water. Similar horizons have sometimes been considered fragipans (Fitzpatrick, 1978), even without the strong signs of pedogenesis (S11) required by the fragipan horizon definition (IUSS Working Group 2015).

- Cryogenic fabrics at the structural aggregate or at microscopic scales, inherited from ice segregation and lensing, can allow the location of the former permafrost table. In particular, the coarse platy structural aggregation observed in all the studied soils is likely cryogenic and indicates ice lensing (Van Vliet-Lanoë, 1998) in the ice-rich transient layer.
- Silt-enriched horizons (S5, S11, S12, S13) can be interpreted as supra-permafrost accumulations (Van Vliet-Lanoë, 1985); they are produced by pervection (silt migration along a freezing front, Bockheim et al., 2006), and percolation of silt-enriched water after frost melt along the pores left by ground ice in the active layer. The abundant silt normally characterizing permafrost soils is produced by cryoweathering associated with freeze-thaw action in the active layer (French, 2011).
- Cryoturbations with drop-shaped involutions (Vandenberghe, 2013) as in S11 and the involutions with flat bottom (Watson and Morgan, 1977; Van Vliet-Lanoë, 1991) found in S13 suggest the presence of an impermeable permafrost table at depth, as there is no impermeable rocky layer below. Thus, they may indicate the depth of the active layer. On coarse materials such as in S11 and S13, a MAAT lower than -8°C should be necessary (Vandenberghe, 2013). Large cryoturbation structures may also indicate liquefaction during degradation of ice-rich permafrost (French et al., 2005; Vandenberghe et al., 2016), but the dimensions of the forms described in these paleosols are not indicative of such processes.
- Evidence of waterlogging or perched water table in what is now a freely drained soil can be considered another indicator of past permafrost conditions (Van Vliet-Lanoë, 1991). Fe redoximorphic features, such as nodules or Fe-oxide coatings, often mark the first few cm above the permafrost table in present-day soils in the arctic tundra (Van Vliet-Lanoë, 1989; Jakobsen et al., 1996, Jones et al., 2010; Gubin and Lupachev, 2017). Placic horizons (S4, S5, with a Fe_{ox} and Fe_d content of, respectively, 18.8-6.5 and 23.1-33.1 g/kg) or Fe-Mn nodule rich layers close to the 2/3 thaw unconformity (S4, S5 with a Fe_{ox} and Fe_d content of, respectively, 8.0-7.7 and 23.1-10.2 g/kg) might thus be interpreted as Fe-Mn accumulation close to a former permafrost table. The placic horizons in S12 could however be easily interpreted as indicators of the observed slow permeability of silt-enriched horizons inside the stratified slope deposit.
- The highly humified organic matter that accumulated sometimes at the bottom of the involutions (S11, S12, S13) or above structural discontinuities (S11) can be interpreted as supra permafrost accumulation of finely grained organic matter derived from cryoturbation and illuviation of soluble organic matter compounds. This is associated with the so-called retinization of humus (accumulation of polymerized and microdivided organic matter on top of the permafrost table, Dimo, 1965; Gubin and Lupachev, 2017). An accumulation of dissolved

organic matter in the intermediate layer (which melts during particularly warm years) that gets sequestered during permafrost aggradation can also be hypothesized (Michaelson et al., 1996).

In Unit 2, the upper stone faces were often covered by thick and dense silt accumulations (silt caps), while pockets of tightly packed small stones and sand grains were filling the spaces created by the gradual disappearance of ice below stones (Fitzpatrick, 1978; Collins and O'Dubhain, 1980). These features evidence intense freeze-thaw processes in Unit 2 in all the studied soils (van Vliet -Lanoë, 1985), and suggest that this layer was located inside a 40 cm (in flat areas) or 105-160 cm thick (in slope soils) active layer for sufficiently long periods. The tiny granular aggregates and sand grains deposited on platy aggregates and in coarse pores sometimes observed in Unit 2 (S5, S18) may also indicate water movement in an active layer (Van Vliet -Lanoë, 1985).

At the same time, the rather abrupt upper boundary of Unit 2, corresponding to radical changes in aggregation, density, and texture, suggests that the same unit has been preserved below the permafrost table for long periods as well. As a consequence, during these climatic phases, the active layer should have been only 40-100 cm thick. Soils in flat areas (S5) likely had a thinner active layer compared to slope soils (S4, S11, S12, S13). Two different climatic regimes, characterized by two main active layer thicknesses, can thus be hypothesized.

The permafrost table normally oscillates in response to annual/decadal or millennial temperature variations. The intermediate layer thus obtained, characterized by the presence of coarse ice lenses, represents the long-term position of the limit between the active layer and the permafrost table (French, 2011). It corresponds to Unit 2 in our soils.

Three sedimentary units/stratigraphic layers characterize the well-studied periglacial cover beds developed in Central Europe (Kleber et al., 2013). The basal layer is dense (more than 1.7 g/cm^3) and composed of residuum of the substrate that underwent solifluction before getting included in permafrost and before loess deposition phases. The intermediate layer has a high loess content and has apparently developed during the Last Glacial Maximum. The Upper Layer, formed during the Late Glacial, has a rather homogeneous thickness (40-70 cm) and is stone-richer than the intermediate layer, but it includes large amounts of loess as well. Thus, many similarities with our Alpine slope soils exist: the almost constant thickness of the upper solifluction layer, the stone orientation along the slope, and the high density of the fragipan-like basal layer (Kleber et al., 2013). Remnants of soils (paleosols) formed during previous interglacial periods have been observed in Switzerland in the intermediate layer (Mailänder and Veit, 2001).

5.2 Pedogenic processes in periglacial conditions and warm interglacials

Many of these soils evidenced a particularly long pedogenic history and a very strong weathering degree throughout Units 1 and 2, sometimes in Unit 3 as well.

For example, S5 has a very fine texture, with more than 20% clay and more than 30% silt in most of the horizons in the central, stone-poor part. Its quartzitic conglomerate substrate is coarse-grained and resistant to weathering, thus it would not easily create such high amounts of fine particles, unless taking into account a very long weathering history (Goodfellow, 2007). The flat morphology inhibited erosion, leading to clay and silt accumulation, which probably made this soil frost susceptible, and able to develop large patterned ground features despite the coarse granulometry of the parent material. The abundance of silt might have been produced by frost shattering and clast abrasion as well (Etzelmüller and Sollid, 1991; Van Vliet-Lanoë, 1998). Moreover, even if no loess has been detected in other relict surfaces with ancient soils (D'Amico et al., 2016), small additions of aeolian materials cannot be excluded. In fact, the development of patterned ground features requires a high heterogeneity of particle size distribution and abundant fines (Van Vliet-Lanoë, 1998). In turn, patterned ground formation and development leads to an additional strong accumulation of fines in the central part (Ugolini et al., 2006; D'Amico et al., 2015).

In S5, the stones on the stony margin have a shape ranging from rounded to angular, which was associated with a soft and hard consistence respectively, related to a contrasting weathering degree (highly weathered rounded clasts, weakly weathered angular ones) and with a differential presence of weathering rinds. The rinds were absent in the unweathered clasts, while they were reddish or dark brown, sometimes layered, and with a thickness between 2 and 25 mm in the weathered ones. The same differences have been detected in the coarse fragments included in the Unit 1 of S4 (solifluction layer) or in cryoturbated layers (Unit 2) of S11 and S13. This random coexistence of stones with contrasting weathering degree implies many cycles of cryoturbation separated by long periods characterized by strong weathering in a non-periglacial climate, evidencing a particularly old soil/surface age. It is important to underline that mixing of such differently weathered materials is impossible in present-day climatic conditions.

If we consider Unit 1 as a solifluction sheet activated during the late glacial ca. 11500 years ago, as it is in Central European cover beds, we can interpret Unit 1 soils as formed during the Holocene. Their pedogenic degree is, in fact, similar to the soils normally observed in the study area outside relict surfaces (Catoni et al., 2016; Stanchi et al., 2017; Pintaldi et al., 2018; Bonifacio et al., 2018). Below, Unit 2 on slopes usually included well preserved, though cryoturbated, Podzolic paleosols, which showed a much stronger pedogenic degree than surface Holocene soils. The thickness, cementation, TOC and Fe-Al contents (Electronic annex) of Bsm horizons and the high weathering

543 degree of E materials indicate that these paleosols required a much longer period or much stronger
544 pedogenic environments for their development, likely during warm interglacials.
545 In particular, the pedogenic development degree observed in Unit 2 and, sometimes, in Unit 3, is
546 not compatible with the short period of time between the end of the LGM and the Younger Dryas
547 (Late Glacial, lasted around 2000 years). It is well known, in fact, that fully developed Podzols
548 normally form in 1000-3000 years, while shorter periods are required in extremely wet climates or
549 on sands (Sauer et al., 2007). In the environmental conditions characterizing the study area (average
550 precipitation lower than 1200 mm/y and broadleaf vegetation), the time required cannot be shorter.
551 The slow podzolization rate well agrees with the weak development of Podzols observed in Unit 1.
552 The reddish clay cutans observed in deep layers (e.g. the Crt horizon in profile S18) indicate that
553 soils underwent rubification and clay translocation (lessivage) during some phases of their
554 development, which evidence very different environmental conditions compared to the present-day
555 podzol-forming environment. The same processes (illuviation of rubified clay cutans) have already
556 been observed in deep horizons of extremely well developed podzolic soils in the study area
557 (D'Amico et al., 2016). These Bts horizons were usually located below cemented ortstein Bsm
558 ones, which thus inhibit the water percolation necessary for clay illuviation. These processes require
559 particularly long time frames. While clay lessivage is visible in Late Pleistocene Italian soils,
560 rubification is normally observed in at least Middle Pleistocene ones (Carnicelli and Costantini,
561 2015; Sauer, 2010).
562 The particularly good preservation of pedogenic horizons in the second layer, despite the
563 cryoturbation structures (drop-shaped involutions, wedges, detached organic matter-rich materials
564 translocated at depth) remains problematic to understand, particularly in consideration of the
565 sloping terrain. According to Van Vliet-Lanoë (1998), pedofeatures inherited from previous
566 pedogenesis might be preserved during frost periods only below the depth of seasonal frost
567 penetration or in parts of the active layer which are desiccated in winter. However, the well
568 recognizable permafrost table, the involutions, the translocated organic matter-rich aggregates etc.
569 evidence that none of the two hypothesis can be considered to explain the preservation of Unit 2 in
570 our soils.
571 The modified Profile Development Index PDI (Harden 1988) confirms a strong pedogenic degree,
572 particularly if compared with published data of other soils of area. The modified PDI index of these
573 polygenetic soils (31-64, table 5) is comparable with paleosols developed on relict flat surfaces
574 (D'Amico et al., 2016), which had values ranging between 27 and 80. Common soils in the Tanaro
575 Valley (Catoni et al., 2016) developed on surfaces lacking clear Pleistocene periglacial
576 morphologies had much lower values, ranging between 0 (Regosols) and 14 (Podzols).

Only Luvisols, which require many thousands of years for their development (Carnicelli and Costantini, 2015), and Podzols had values above 10, comparable therefore to the soils developed in the surface Unit in our polygenetic profiles. Soils preserved in deeper layers often had much higher values, evidencing a longer time for their formation.

Conclusions

Many soil indicators associated with ice lensing, cryoturbation, and permafrost are preserved in the studied soils, such as soil wedges, structural discontinuities with platy aggregation and vesicular structure, silt migration, strong lateral textural and granulometric sorting, drop-shaped involutions, buried organic matter-rich horizons, soil wedges. The topographical effects of frost action on soils (such as large-scale sorted patterned ground, blockstreams and blockfields, stratified slope deposits, thick solifluction/gelifluction lobes) suggest the presence of widespread permafrost as well. The active layer thickness was probably 40-100 cm for long times, but apparently deepened to 105-160 cm in other long periods.

A 20°C colder climate than today has been hypothesized in England (Ballantyne and Harris, 1994). A temperature depression of only 4-6°C has been assumed in Continental Europe, based on the 1000 m snow-line variation between the LGM and present-day (Ballantyne and Harris, 1994), but a greater difference in temperature is more probable, given the much lower precipitation rate characterizing glacial periods.

Moreover, there are numerous well-preserved permafrost soil indicators in French lowlands (Bertran et al., 2014), evidencing a temperature at least 10-12°C lower than today during the LGM (French, 2007). If similar conditions were encountered in the Western Alps, it means that the MAAT in the study area could have been as low as -6°C. Such a low MAAT is compatible with most of the observed surface and soil periglacial fossil features. Our results, thus, can give important insights in paleoclimatic reconstruction for the Western Mediterranean and the Alpine regions.

References

André, M.F., Hall, K., Bertran, P., Arocena, J., 2008. Stone runs in the Falkland Islands: periglacial or tropical? Geomorphology 95, 524-543.

Ballantyne, C.K., Harris, C., 1994. The periglaciation of Great Britain. Cambridge University Press, Cambridge, UK.

Ballantyne, C.K., 2010. A general model of autochthonous blockfield evolution. Permafrost Periglac. Proc. 21, 289-300.

612 Ballantyne, C.K., 2013. Patterned ground. In: eds. Elsevier. Encyclopedia of Quaternary Science,
613 vol. 3, 452-463.
614 Benedict, J.B., 1970. Frost Cracking in the Colorado Front Range. Geogr. Ann. Ser. A-phys. Geogr.
615 52(2), 87-93
616 Benedict, J.B., 1979. Fossil ice-wedge polygons in the Colorado Front Range: origin and
617 significance. Geological Society of America Bulletin, Part I, 90,173-180.
618 Bertran, P., Andrieux, E., Antoine, P., Coutard, S., Deschodt, L., Gardère, P., Hernandez, M.,
619 Legentil, C., Lenoble, A., Liard, M., Mercier, N., Moine, O., Sitzia, L., Van Vliet-Lanoë, B., 2014.
620 Distribution and chronology of Pleistocene permafrost features in France: database and first results.
621 Boreas 43, 699-711.
622 Biancotti, A., G. Bellardone, S. Bovo, B. Cagnazzi, L. Giacomelli & C. Marchisio. 1998.
623 Distribuzione regionale di piogge e temperature . Regione Piemonte, Collana Studi Climatologici in
624 Piemonte, 1. Regione Piemonte, Università degli Studi di Torino, Torino.
625 Bockheim, J.G., Mazhitova, G., Kimblr, J.M., Tarnocai, C., 2006. Controversies on the genesis and
626 classification of permafrost-affected soils. Geoderma 137, 33-39.
627 Boelhouwers, J.C., 1999. Relict periglacial slope deposits in the Hex River Mountains, South
628 Africa: observations and palaeoenvironmental implications. Geomorphology 30, 245-258.
629 Bonifacio, E., D'Amico, M.E., Catoni, M., Stanchi, S., 2018. Humus forms as a synthetic parameter
630 for ecological investigations. Some examples in the Ligurian Alps (North–Western Italy). Appl.
631 Soil Ecol. 123, 568-571. DOI: japsoil.2017.04.008.
632 Carnicelli S., Costantini E.A., 2013. Time as a Soil Forming Factor and Age of Italian Soils. In:
633 Costantini E., Dazzi C. (eds) The Soils of Italy. World Soils Book Series. Springer, Dordrecht; pp.
634 93-104.
635 Carraro, F., Giardino, M., 2004. Quaternary glaciations in the western Italian Alps – a review. In:
636 Ehlers, J. and Gibbard, P.L. (Eds.) Quaternary Glaciations – Extent and Chronology Part 1: Europe.
637 Elsevier, Amsterdam.
638 Catoni, M., D'Amico, M.E., Zanini, E., Bonifacio, E., 2016. Effect of pedogenic processes and
639 formation factors on organic matter stabilization in alpine forest soils. Geoderma 263, 151–160.
640 Clark, M.G., Ciolkosz, E.J., 1988. Periglacial geomorphology of the Appalachian highlands and
641 interior highlands south of the glacial border - a review. Geomorphology 1,191-220.
642 Collins, J.F., O'Dubhain, T., 1980. A micromorphological study of silt concentraions in some Irish
643 Podzols. Geoderma 24, 215-224.

644 Cremaschi, M., Van Vliet-Lanoë, B., 1990. Traces of frost activity and ice segregation in
645 Pleistocene loess deposits of northern Italy. Deep seasonal freezing or permafrost? Quat. Int. 5, 39–
646 48
647 D'Amico, M.E., Gorra, R., Freppaz, M., 2015. Small-scale variability of soil properties and soil–
648 vegetation relationships in patterned ground on different lithologies (NW Italian Alps). Catena 135,
649 47-58.
650 D'Amico, M.E., Catoni, M., Terribile, F., Zanini, E., Bonifacio, E., 2016. Contrasting
651 environmental memories in relict soils on different parent rocks in the south-western Italian Alps.
652 Quat. Int. 415, 61-74.
653 Dimase, A.C., 2006. Fossil cryogenic features in paleosols of southern Italy: Characteristics and
654 paleoclimatic significance. Quat. Int. 156-157, 32-48.
655 Dimo, V.N., 1965. Formation of a humic-illuvial horizon in soils with permafrost. Sov. Soil Sci. 9,
656 1013-1021.
657 Etzelmüller, B., Sollid, J.L., 1991. The role of weathering and pedological processes for the
658 development of sorted circles on Kvadehuksletta, Svalbard - a short report. Pol. Res. 9(2), 181-191
659 FAO, 2006. Guidelines for Soil Description. fourth ed. FAO, Rome.
660 Federici, P.R., Granger, D.E., Ribolini, A., Spagnolo, M., Pappalardo., M., Cyr, A.J., 2012. Last
661 glacial maximum and Gschnitz stadial in the Maritime Alps according to ^{10}Be cosmogenic dating.
662 Boreas 41, 277-291.
663 Fioraso, G., Spagnolo G., 2009. I block stream del Massiccio Peridotitico di Lanzo (Alpi Nord-
664 occidentali). Il Quaternario It. Journ. Quat. Sc. 22(1), 3-22.
665 Firpo, M., Guglielmin, M., Queirolo, C., 2006. Short Communication. Relict blockfields in the
666 Ligurian Alps (Mount Beigua, Italy). Permafrost Periglacial Process. 17, 71-78.
667 Fitzpatrick, E.A., 1956. An indurated soil horizon formed by permafrost. J. Soil Sci. 7(2), 248-257.
668 Fitzpatrick, R.W., 1978. Periglacial soils with fossil permafrost horizons in southern Africa. Ann.
669 Natal Mus. 23(2), 475-484.
670 French, H.M., Demitroff, M., Forman, S.L., 2005. Evidence for Late-Pleistocene thermokarst in the
671 New Jersey Pine Barrens (Latitude 39° N), Eastern USA. Permafrost Periglac. Process. 16, 173-
672 186.
673 French, H.M., 2007. The periglacial environment, third ed. Wiley, Chichester, UK, 458 pp.
674 French, H.M., Shur, Y., 2010. The principles of cryostratography. Earth Sci. Rev. 101, 190-206.
675 French, H.M., 2011. Frozen sediments and previously frozen sediments. In: Martini, I.P., French,
676 H.M., Pérez Alberti, A. (eds), Ice marginal and periglacial processes and sediments. Geological soc.
677 London, Special Publication, 354, pp. 153-166.

678 Goldthwait, R.P., 1976. Frost sorted patterned ground: a review. Quat. Res. 6, 27-35.
679 Goodfellow, B.W., 2007. Relict non-glacial surfaces in formerly glaciated landscapes. Earth Sci.
680 Rev. 80, 47-73.
681 Grab, S., 2002. Characteristics and paleoenvironmental significance of relict sorted patterned
682 ground, Drakensberg plateau, Southern Africa. Quat. Sci. Rev. 21, 1729-1744.
683 Gubin, S.V., Lupachev, A.V., 2017. Soils of loamy watersheds of coastal tundra in the north of
684 Yakutia: pedogenic conditions and processes. Eurasian Soil Sci. 50(2), 133-141.
685 Guglielmin, M., Notarpietro, A., 1997. Il permafrost alpino. Concetti, morfologia e metodi di
686 individuazione. Quaderni di Geodinamica Alpina e Quaternaria 5, Centro di Studio per la
687 Geodinamica Alpina e Quaternaria, Chiavenna.
688 Harris, S.A., 1994. Climatic zonality of periglacial landforms in mountain areas. Arctic 47(2), 184-
689 192.
690 Jakobsen, B. H., Siegert, C., Ostroumov V., 1996. Effect of Permafrost and Palaeo-Environmental
691 History on Soil Formation in the lower Kolyma Lowland, Siberia. Danish Journ. of Geogr. 96, 40-
692 50, 1996.
693 Harden, J.W., 1982. A quantitative index of soil development from field descriptions: examples
694 from a chronosequence in central California. Geoderma 28, 1-28.
695 Harden, J.W., Taylor E.M., 1983. A quantitative comparison of soil development in four climatic
696 regimes. Quat. Res. 20, 342-359.
697 IUSS Working Group WRB, 2015. World Reference Base for Soil Resources 2014, update.
698 International soil classification system for naming soils and creating legends for soil maps. World
699 Soil Resources Reports No. 106. FAO, Rome.
700 Jones, A., Stolbovoy, V., Tarnocai, C., Broll, G., Spargaaren, O., Montanarella, L., 2010. Soil Atlas
701 of the Northern Circumpolar Region. European Commission, Publications Office of European
702 Union, Luxembourg.
703 Karte, J., 1983. Periglacial Phenomena and their Significance as Climatic and Edaphic Indicators.
704 GeoJournal 7(4), 329-340.
705 Kleber, A., Müller, S., Terhorst, B., Thiemeyer, H., 2013. Genesis of cover beds. In: Kleber, A.,
706 Terhorst, B., (Eds.), Developments in Sedimentology 66: Mid-Latitude Slope Deposits (Cover
707 Beds). Elsevier, Amsterdam, pp. 38-57.
708 Mailänder, R., Veit, H., 2001. Periglacial cover-beds on the Swiss Plateau: indicators of soil,
709 climate and landscape evolution during the Late Quaternary. Catena 45, 251-272.
710 Matsuoka, N., 2011. Climate and material controls on periglacial soil processes: towards improving
711 periglacial climate indicators. Quat. Res. 75, 356-365.

712 Michaelson, G.J., Ping., C.L., Kimble, J.M., 1996. Carbon storage and distribution in tundra soils of
713 Arctic Alaska, U.S.A.. Arct. Alp. Res. 28(4), 414-424.
714 Murton, J.B., Kolstrup, E., 2003. Ice-wedge casts as indicators of palaeotemperatures: precise proxy
715 or wishful thinking? Prog. Phys. Geogr. 27, 155–170.
716 Paro, L., 2011. Il ruolo dei processi criotici nell'evoluzione del paesaggio alpino: il caso di studio
717 dei block stream del Complesso Ultrabasico di Lanzo (Alpi occidentali italiane). Relationship
718 between cryotic processes and block streams evolution in the Lanzo Ultrabasic Complex (Western
719 Italian Alps). Ed. Arpa Piemonte, Torino.
720 Peterson, R.A., Krantz, W.B., 2008. Differential frost heave model for patterned ground formation:
721 Corroboration with observations along a North American arctic transect. J. Geophys. Res. 113,
722 G03S04.
723 Pintaldi, E., D'Amico, M.E., Stanchi, S., Catoni, M., Freppaz, M., Bonifacio, E., 2018. Humus
724 forms affect soil susceptibility to water erosion in the Western Italian Alps. App. Soil Ecol. 123,
725 478-483. DOI: j.apsoil.2017.04.007
726 Prosser, I.P., Roseby, S.J., 1995. A chronosequence of rapid leaching of mixed podzol soil materials
727 following sand mining. Geoderma 64, 297-308.
728 Rea, B.R., 2013. Blockfields (Felsenmeer). In: Elias, S.A., (ed.), The Encyclopedia of Quaternary
729 Science 3, Elsevier, Amsterdam, pp. 523-534
730 Rellini, I., Firpo, M., Martino, G., Riel-Salvatore, J., Maggi, R., 2013. Climate and environmental
731 changes recognized by micromorphology in Paleolithic deposits at Arene Candide (Liguria, Italy).
732 Quat. Int. 315, 42-55.
733 Rellini, I., Trombino, L., Rossi, P.M., Firpo M., 2014. Frost activity and ice segregation in a
734 palaeosol of the Ligurian Alps (Beigua Massif, Italy): Evidence of past permafrost? Geogr. Fis.
735 Dinam. Quat. 37, 29-42.
736 Šamonil, P., Daněk, P., Schaetzl, R.J., Vašičkovà, I., Valtera, M., 2015. Soil mixing and genesis as
737 affected by tree uprooting in three temperate forests. Eur. J. Soil. Sci 66, 589-603.
738 Sauer, D., 2010. Approaches to quantify progressive soil development with time in Mediterranean
739 climate—I-use of field criteria. J Plant Nutr Soil Sci 173(6), 822–842.
740 Schaetzl, R.J., Mokma, D.L., 1988. A numerical index of Podzols and Podzolic soil development.
741 Phys. Geogr. 9, 232-246.
742 Schaetzl, R.J., Anderson, S., 2005. Soils Genesis and Geomorphology. Cambridge Univ. Press, pp.
743 573-578.

744 Stanchi, S., Catoni, M., D'Amico, M.E., Falsone, G., Bonifacio, E. 2017. Liquid and plastic limits
745 of clayey, organic C-rich mountain soils: Role of organic matter and mineralogy. Catena 151, 238-
746 246.
747 Ugolini, F.C., Corti, G., Certini, G., 2006. Pedogenesis in the sorted patterned ground of Devon
748 Plateau, Devon Island, Nunavut, Canada. Geoderma 136, 87–106.
749 Van Reeuwijk, L.P., 2002. Procedures for Soil Analysis. Technical Paper n. 9. International
750 Soil Reference and Information Centre, Wageningen, Netherlands.
751 Van Steijn, H., Boelhouwers, J., Harris, S., Hétu, B., 2002. Recent research on the nature, origin
752 and climatic relations of blocky and stratified slope deposits. Progr. Phys. Geogr. 26(4), 551-575.
753 Van Vliet-Lanoë, B., 1985. Frost effects in soils. In: Boardman, J. (ed.), Soil and Quaternary
754 Landscape Evolution. Wiley, Chichester, pp. 117-158.
755 Van Vliet-Lanoë, B., 1989. Dynamics and extent of the Weichselian permafrost in Western Europe
756 (substage 5E to stage 1) Quat. Int. 3-4, 109-113.
757 Van Vliet-Lanoë, B., 1991. Chronostratigraphy and paleoclimatic meaning of cryogenic
758 deformation in the Central European loess. GeoJournal 24(2), 157-163.
759 Van Vliet-Lanoë, B., 1998. Frost and soils: implications for paleosols, paleoclimates and
760 stratigraphy. Catena 34, 157-183.
761 Vandenberghe, J., 2013. Cryoturbation structures. In: n: Elias, S.A., (ed.), The Encyclopedia of
762 Quaternary Science 3, Elsevier, Amsterdam, pp. 430-435.
763 Vandenberghe, J., Pissart, A., 1993. Permafrost changes in Europe during the Last Glacial.
764 Permafrost Periglacial Process. 4, 121–135.
765 Vandenberghe, J., Wang, X., Vandenberge, D., 2016. Short Communication. Very large
766 cryoturbation structure of Last Permafrost Maximum age at the foot of the Qilian Mountains (NE
767 Tibet Plateau, China). Permafrost Periglacial Process. 27, 138-143.
768 Vanossi, M., 1990. Alpi Liguri: 11 Itinerari. Guide Geologiche Regionali. BE-MA, Pavia.
769 Watson, E., Morgan, A.V. 1977. The periglacial environment of Great Britain during the Devensian
770 [and discussion]. Philosophical Transactions of the Royal Society of London, B, 280, 183-198.
771 Wilson, P., 2013. Blockfields (Felsenmeer). In: Elias, S.A., (ed.), The Encyclopedia of Quaternary
772 Science 3, Elsevier, Amsterdam, pp. 523-534
773

Figure captions

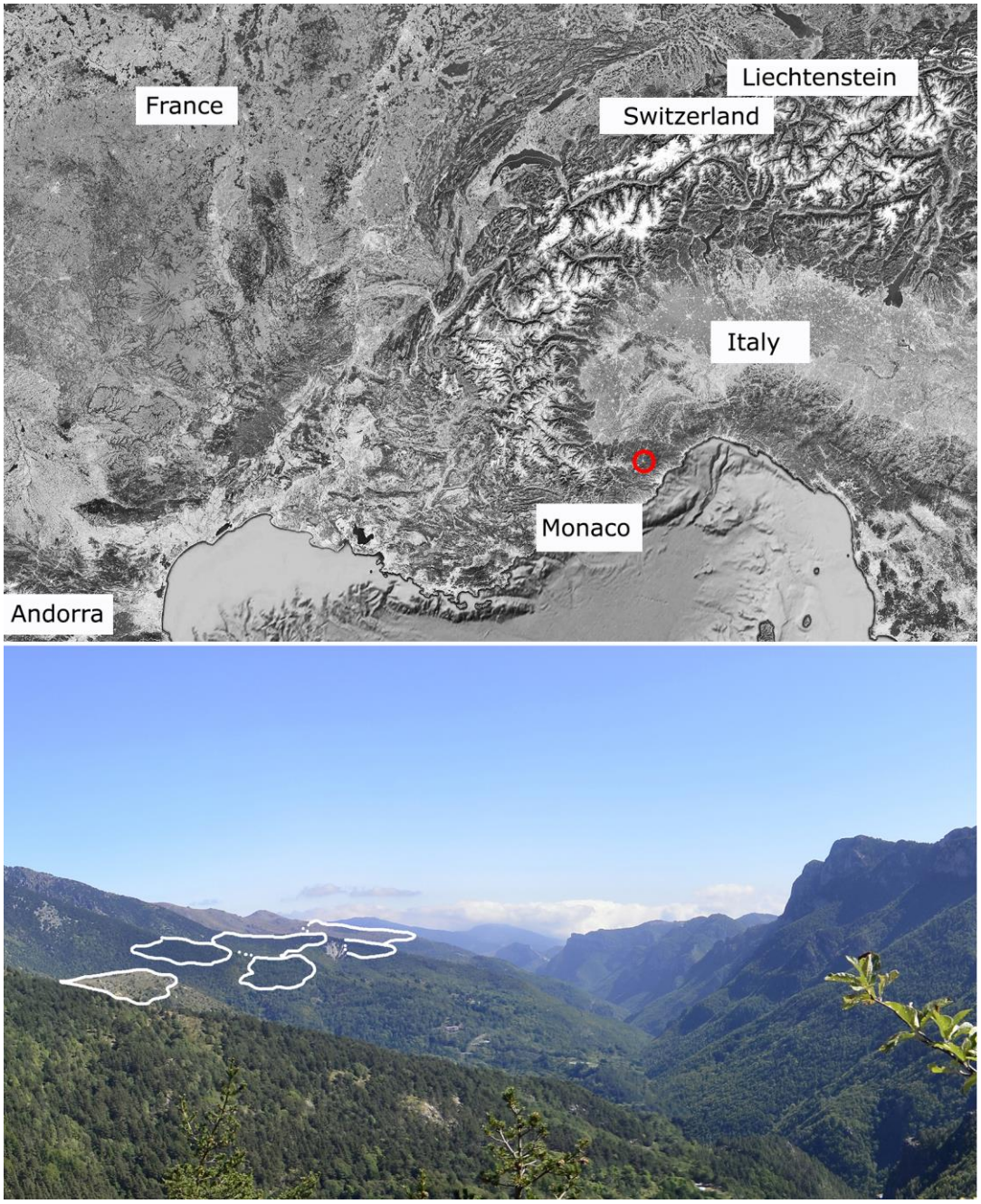

Fig. 1: The study area in the Ligurian Alps and some of the relict surfaces considered.

Fig. 2: Soils with fragipan showing a different number of structural discontinuities. a) profile D1, Eutric Skeletic Fragic Retisol (Loamic); b) profile S18, Retic Albic Ortsteinic Podzol (Fragic, Hyperspodic).

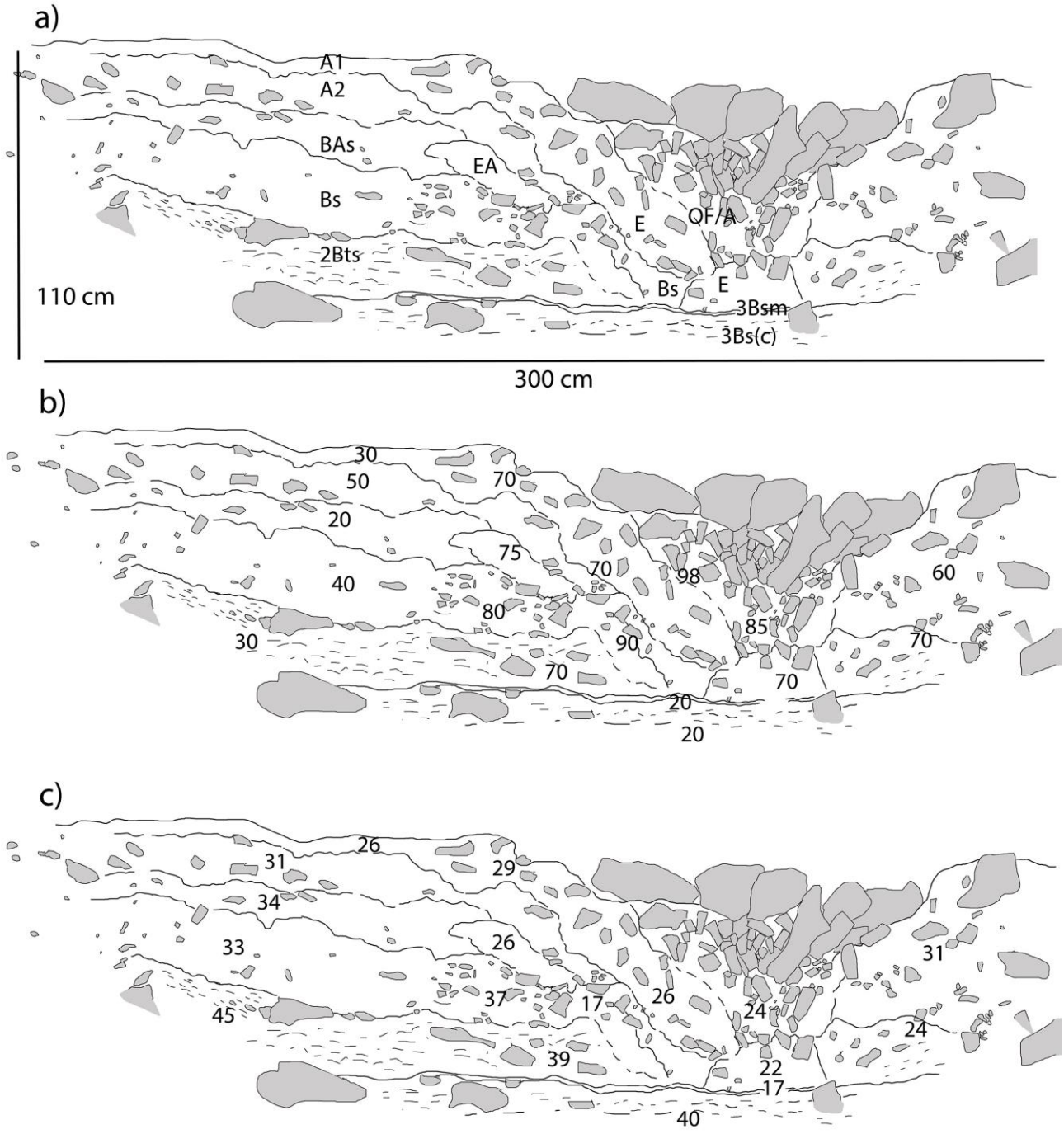

781

782 Fig. 3: S5, Skeletic Umbric Entic/Albic Podzol (Abruptic, Loamic, Densic, Relictiturbic), located in
783 a large-scale sorted patterned ground flat area; a) - genetic horizon; b) – stone fragment (%); c) –
784 silt content (%).

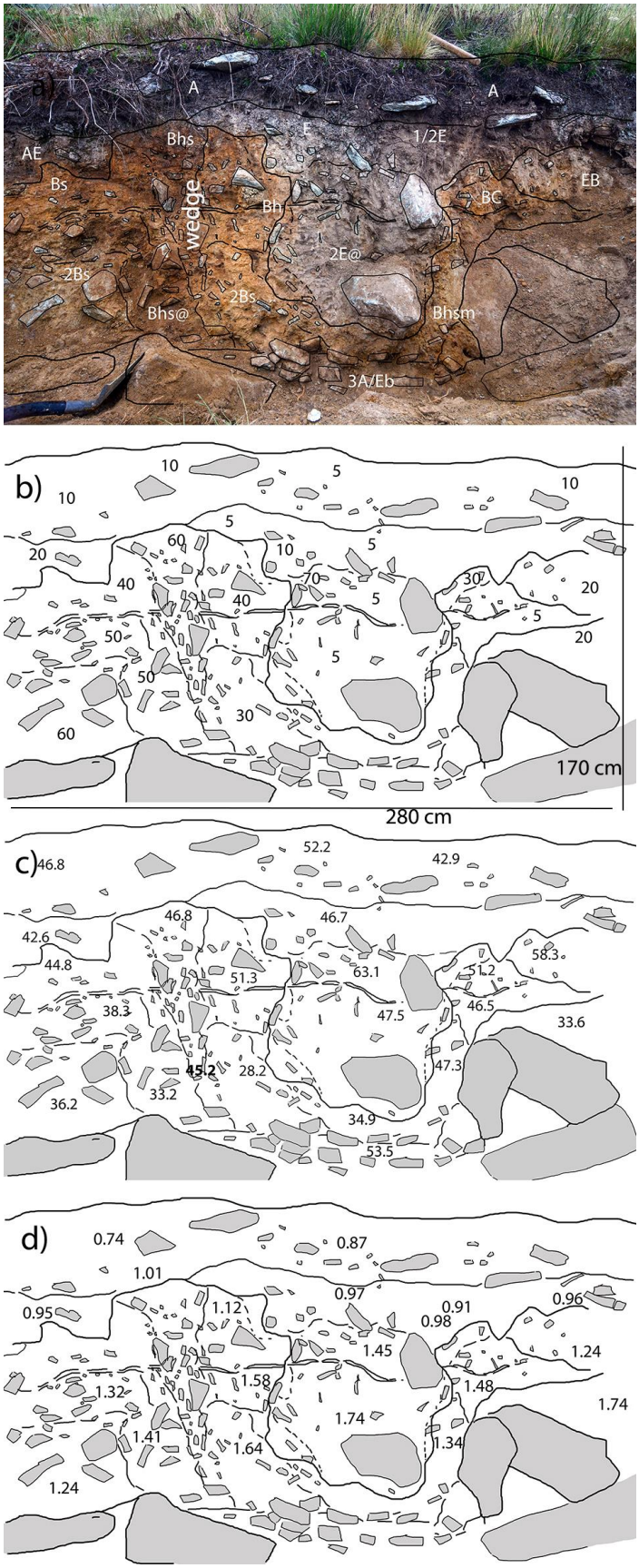

Fig. 4: S11, Albic Podzol (Loamic, Densic, Ruptic, Relictiturbic), showing a large scale drop-like inclusion and a wedge cast (a); stone (v/v, b) and silt (w/w, c) percentages in the different horizons, and bulk density (g/cm^3, d).

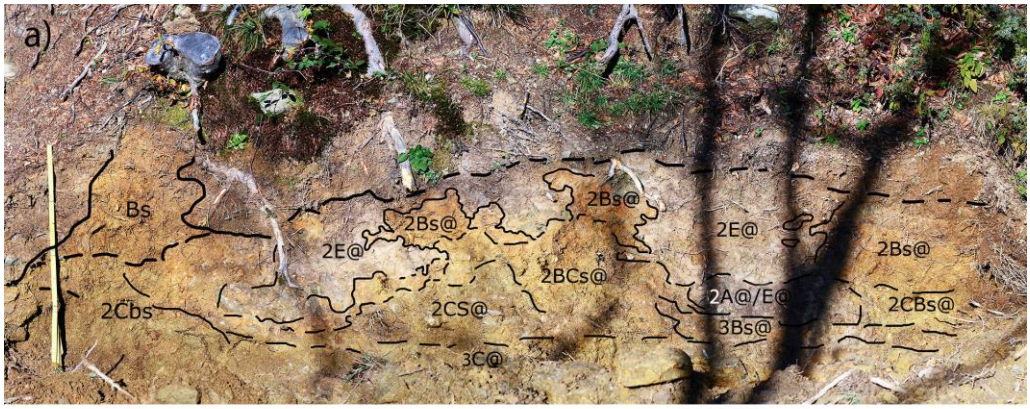
a)
Bs
2Cbs
2E@
2Bs@
2Bs@
2BCs@
2CS@
3C@
2E@
2A@/E@
3Bs@
2Bs@
2CBs@

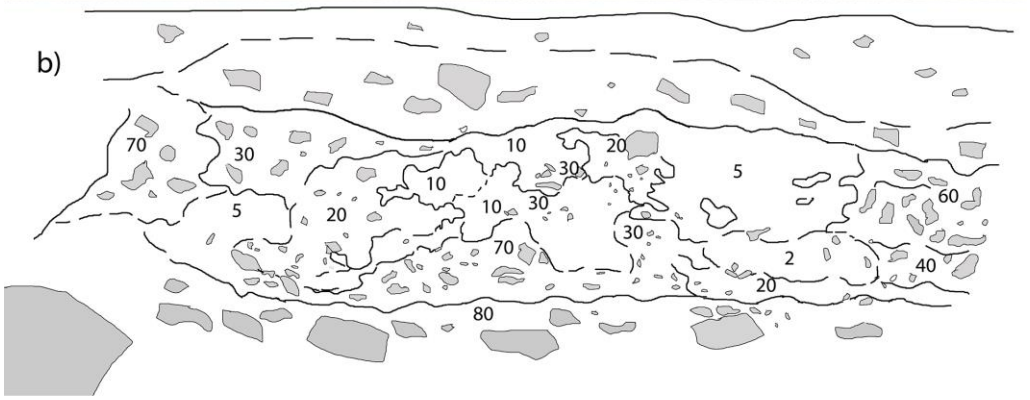
b)
70
30
5
20
10
10
10
30
30
70
80
20
5
30
2
20
60
40

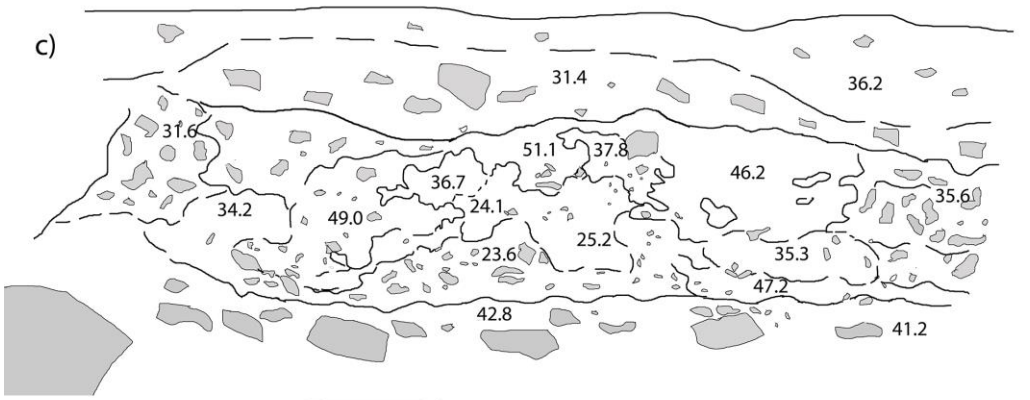
c)
31.6
34.2
49.0
36.7
24.1
51.1
37.8
31.4
23.6
25.2
42.8
46.2
36.2
35.6
35.3
47.2
41.2

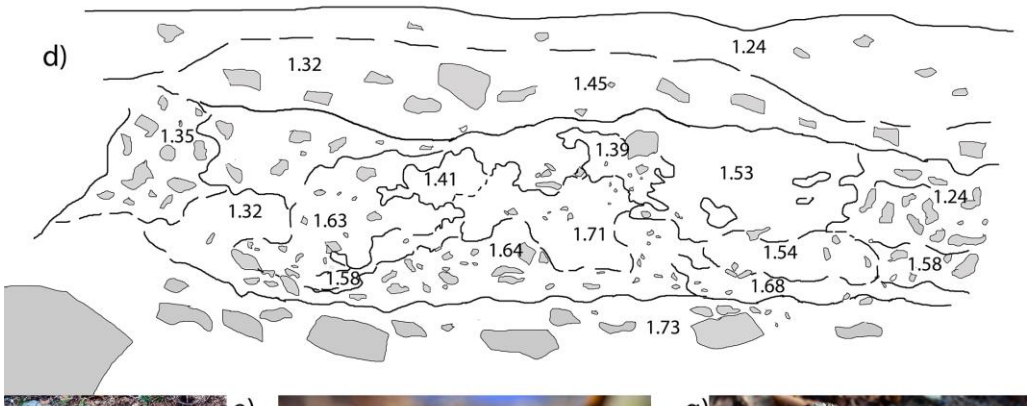
d)
1.35
1.32
1.32
1.63
1.41
1.45
1.64
1.58
1.39
1.71
1.73
1.53
1.54
1.68
1.24
1.24
1.58


e)


f)


g)

Fig. 5: S13, Albic Podzol (Loamic, Densic, Ruptic, Relictiturbic) with convoluted cryoturbated horizons and drop-like inclusions (a); stone (v/v, b) and silt (w/w, c) percentages in the different horizons, and bulk density (g/cm^3, d); Holocene Podzol above the stone-rich 2Bs@ horizon, on the right of the profile (e); organic-matter rich, platy aggregate in the 2A@/2E@ horizon (f); E and Bs horizon material in the convoluted area between the 2Bs@ and the 2E@ horizons (g).

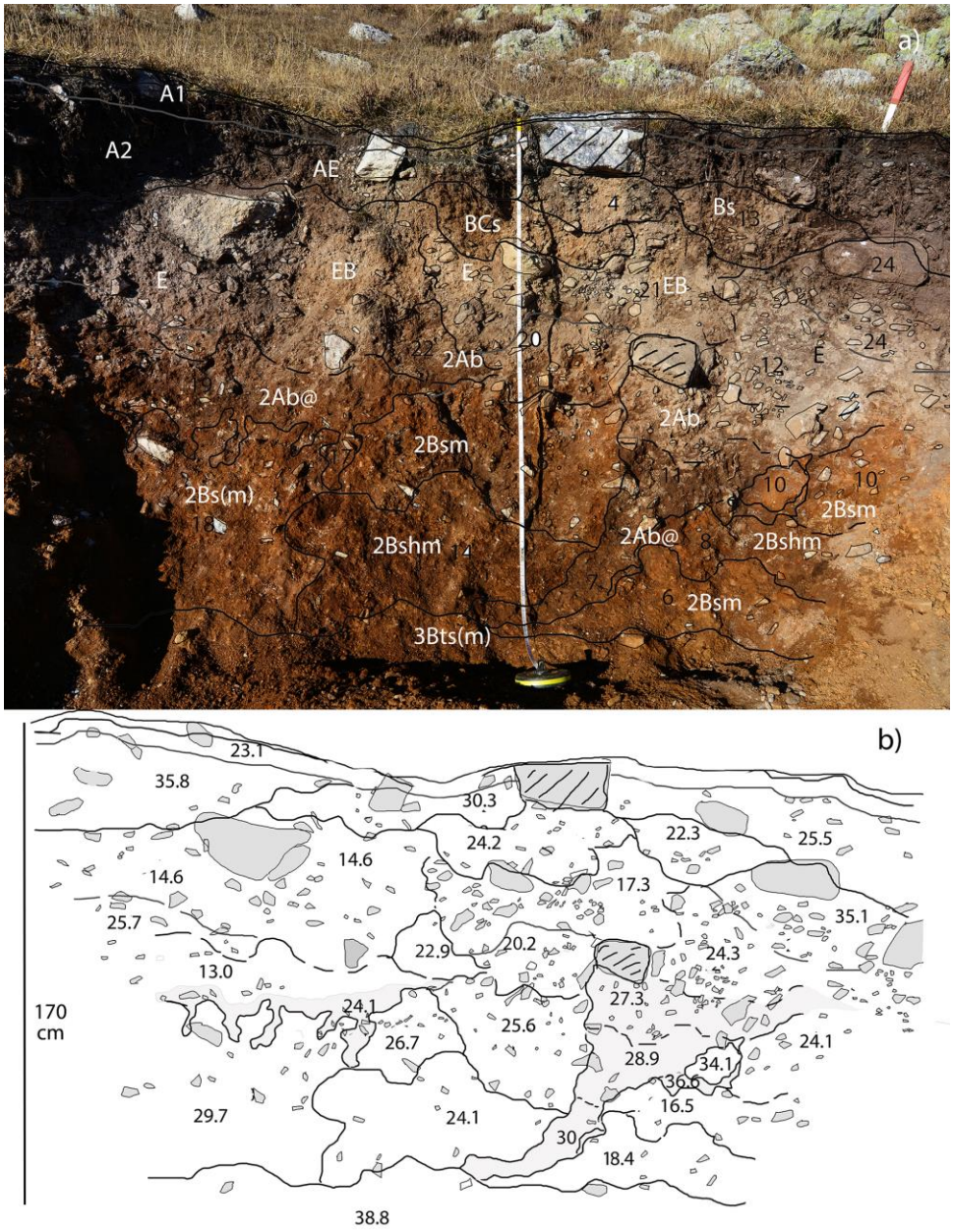

Fig. 6: S4, Hyperskeletic Umbric Albic Ortstenic Podzol (Densic, Ruptic, Hyperspodic Relictiturbic) with small convolutions below the base of Unit 1 and wedge casts (6a); widely varying silt content in the different horizons (fig. 6b)

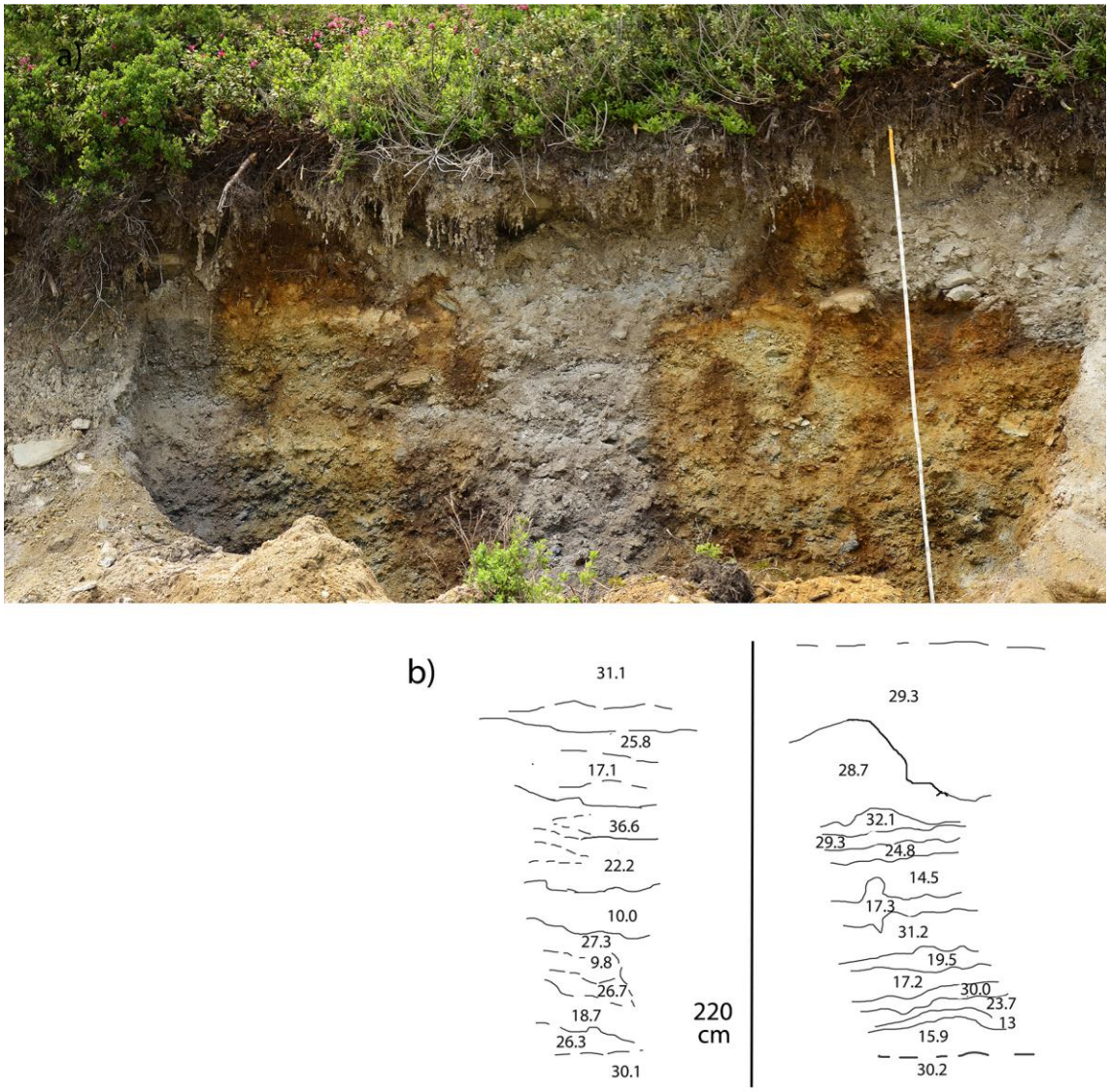

807

808 Fig7 S12: Hyperskeletic Glossic Umbric Hyperalbic Ortstenic Podzol (Densic, Ruptic, Hyperspodic
809 Relictiturbic) developed in stratified slope deposits (grèzes litées), showing discontinuous
810 pedogenic horizons (a) and a stratification of silt or stone rich layers (b).

811

812

Table 1: location and environmental properties of the selected soils. The substrate lithology is from Vanossi (1990).

Main cryogenic characteristic	Soil	Site	Altitude m a.s.l.	Slope steepness	Vegetation cover	Substrate lithology	Landform
Fragipan	D1	Ormea	730	10°	*Ostrya carpinifolia* forest	Shales	Cryoturbated slope
Fragipan	S18	Colma di Casotto (Garessio)	1480	4°	*Fagus sylvatica* forest	Quartzitic conglomerate (“Porfiroidi del Melogno”	Cryoplanation surface
Sorted patterned ground	S5	La Colma (Ormea)	1500	1°	Grazed grassland/heath	Quartzitic conglomerate ("Verrucano Brianzonese")	Cryoplanation surface / relict terrace
Unsorted patterned ground / dropsoils / cryoturbations	S11	Colma di Casotto (Garessio)	1695	3°	Grazed grassland/heath	Ortogneiss	Cryoplanation surface
Unsorted patterned ground / dropsoils / cryoturbations	S13	Colma di Casotto (Garessio)	1595	12°	*Fagus sylvatica* forest	Ortogneiss	Cryoturbated slope
Stone-banked solifluction lobe / soil wedge casts	S4 - PLC	La Colma (Ormea)	1620	15	Grazed grassland/heath	Quartzitic conglomerate ("Verrucano Brianzonese")	Cryoturbated slope
Stratified slope deposit (greze litees)	S12 - superwedge	Colma di Casotto (Garessio)	1470	8°	*Fagus sylvatica* forest	Quartzitic conglomerate (“Porfiroidi del Melogno”	Cryoturbated slope

Table 2: The periglacial surface morphologies observed at the study sites, and their paleoenvironmental significance according to the available literature.

Periglacial features	Site	Indicator of	Environmental conditions	Notes/observations	References
Blockfields/blockstreams	D1, S18, S5	Indicators of permafrost even if a previous, intense weathering of the materials in warm and humid climates is usually required	- MAAT below -6°C and precipitations below 500 mm - sometimes deep seasonal freezing	-	Harris, 1994; Rea, 2013; Wilson, 2013; André et al., 2008; Boelhouwers, 1999
Large scale sorted patterned ground (circles and stripes > 1 m ca.)	S5, S11, S13, S12	Indicative of permafrost conditions	- MAAT lower than 0/-4°C, when developed in well drained areas and in absence of a shallow impermeable layer. - Active forms are presently found at MAAT below -1.6 °C - In the Alps, active large sorted patterned ground morphologies are active above ca. 2700 m of elevation, which corresponds to a MAAT of more or less -3°C	-In the Alps it seems that the patterned ground wider than 0.8 m is developed above permafrost - Sorted patterned ground width and depth of sorting can indicate the depth of the active layer (e.g. 2 m diameter of a sorted circle indicates a 60-70 cm thick active layer)	Matsuoka, 2011; Goldthwait, 1976; Karte, 1983; Ballantyne, 2013; French, 2007; Grab, 2002; D'Amico et al., 2015; Guglielmin and Notarpietro, 1997; Ballantyne and Harris, 1994; Peterson and Krantz, 2008
Rock glaciers	D1	Landform normally associated with sporadic permafrost conditions in a rather continental climate	mean annual precipitation below 1200 mm	-	Karte, 1983
Tors	S18	Usually associated with periglacial morphogenesis (solifluction and cryoplanation)	-	Their formation and the precise relation with periglacial environment and the time required for their development is under debate	Ballantyne and Harris, 1994

Grèzes litées (Stratified slope deposits)	S12	Periglacial processes such as solifluction and gelifluction	-	The severity of their formation environment is under debate	van Steijn et al., 2002
Thick solifluction layers and periglacial cover beds	S4, S11, S12, S13, S18, D1	Permafrost or deep seasonal freezing conditions	-	- if the solifluction layers is thicker than 40 cm, they may indicate annual freeze-thaw cycles, otherwise mostly daily cycles; - when the thickness is up to 150 cm, and layers are mostly undisturbed, they indicate the presence of an ice-rich layer at the top of the permafrost table, over which thick soil mantles slide because of gelifluction	Matsuoka, 2011

820
821
822 Table 3: properties used for the calculation of the Modified PDI inde1 for each horizon type. Aspecific properties, derived from aspecific processes,
823 where used for all types of genetic horizons, while other specific ones were used only for corresponding genetic horizons.

	Aspecific processes/properties				Specific processes/properties					
	Rubification	Texture	Lightening	weathering	redoximorphic	clay films	melanization	E contrast	POD	cementation
A	x	x	x	x			x			
AE/EA	x	x	x	x			x	x		
AC	x	x	x	x			x			
AB	x	x	x	x			x			
E	x	x	x	x	x			x		
EB	x	x	x	x	x			x	x	
Bhs	x	x	x	x	x	x	x		x	x
Bs	x	x	x	x	x	x			x	x
Bw/Bt	x	x	x	x	x	x				

BC	x	x	x	x	x	x				
C	x	x	x	x	x					

824
825
826 Table 4: cryogenic structures and indicators in studied soils.

Soil	Large scale sorted circles or stripes (diameter/width, m)	Blockfield	Blockstream (distance, m)	Tors (distance, m)	Solifluction lobes (height, m)	Covered thickness (m)	Grèzes litées	Cryoturbation structures (types, amplitude, m)	Ice/soil wedge (width*depth, m)	Fragipan/dense layer with platy structure (depth of upper limit, m); 2 depths are shown when 2 dense layers were observed.	SOM-rich cryoturbations (depth, m)	Fe-rich layers (placic horizons / nodules, depth, m)	Verticalized stones, location
D1			50			0.55				0.40			1, fragipan
S18						0.50				0.65 – 0.90 / 1.20			
S5	2-5	1		20						0.45 – 0.90		Placic: 0.90 Nodules: 0.92	1, stony borders
S11			50			0.60		Large scale involutions, >0.8	0.20*0.90	0.60 – 1.60	0.70 - 1.10 (patches of translocated surface horizons); 60/68 (thin Bh layer)	/	1, border between diapirs and surrounded horizons
S13						0.80-1.20		Large scale involutions, drop-shaped, 0.7		1.20 – 2.10	1.20		
S4			15		0.8	1		Small-scale involutions, wedges, 0.2	0.2*1.1	0.50 - 1.60	1.2 – 1.6 (wedge infilling)	Placic: 1.10; nodules: 1.60	
S12			15			0.80	1			0.80	1.70; 2.15 – 2.40, disrupted, buried OF	Placic: 0.80	

827

Table 5: PDI inde1 values of the considered soil profiles compared to common soils (*) (Catoni et al., 2016) and paleosols (**) (D'Amico et al., 2015) observed in the study area.

	PDI whole profile	PDI Surface Unit			PDI other profiles
				P1*	11.14
S13	44.44	14.88		P2*	0
				P3*	4.46
S11	31.07	16.39		P9*	2.85
S5	31.48			P10*	2.68
				P11*	3.53
S4	47.88	9.99		P12*	0.22
D1	63.77			P13*	14.3
S12	42.81			P17*	2.68
S18	46.24			ALB**	44.78
				ORT**	79.58
				PLC**	27.13